Detection of single nucleotide polymorphisms using a DNA Holliday junction nanoswitch—a high-throughput fluorescence lifetime assay

Colin D. McGuinness,*[a] Mira K. Y. Nishimura,[a] David Keszenman-Pereyra,†[b] Paul Dickinson,[b] Colin J. Campbell,[b] Till T. Bachmann,[b] Peter Ghazal[b] and Jason Crain[ac]

Received 9th July 2009, Accepted 21st September 2009
First published as an Advance Article on the web 19th October 2009
DOI: 10.1039/b913455g

We report a simple DNA sensor device, using a combination of binding and conformational switching, capable of rapid detection of specific single nucleotide polymorphisms in an unlabelled nucleic acid target sequence. The detection is demonstrated using fluorescence lifetime measurements in a high-throughput micro plate reader instrument based on the time-correlated single-photon counting technique. The sensor design and instrumental architecture are capable of detecting perturbations in the molecular structure of the probe–target complex (which is similar to that of a Holliday junction), due to a single base pair mismatch in a synthetic target. Structural information, including fluorophore separations, is obtained using time-resolved Förster resonance energy transfer between two fluorophores covalently bound to the probe molecule. The two probes required are designed to detect a single nucleotide polymorphism from a sequence present on each of the two copies of human chromosome 11.

Introduction

Fluorescence techniques are commonly used in high-throughput screening applications and assay development,[1] due to their significant advantages over more traditional techniques such as radiometrics. Namely, fluorescence techniques do not require the disposal of radioactive materials, the materials possess greater shelf life, and an increase in the stability of reagents. Fluorescence lifetime measurements offer additional advantages over fluorescence intensity type measurements in that the technique is concentration independent, artefacts can be easily discriminated against and it is inherently more sensitive, even improving on the sensitivity of time-resolved Förster resonance energy transfer (TR-FRET) assays.

Although the comparison of two human genomes identifies a <0.1% heterozygosity,[2] each human possesses some 3.2 million differences in their diploid genome, most of which are due to single base substitution polymorphisms or more popularly known as single nucleotide polymorphisms (SNPs). Only a minority of these substitutions have any biological significance, and are the basis for human diversity.[3] SNPs can be used as genetic markers, can follow inheritance patterns of chromosomal regions and are useful in the investigation of genetic factors associated with human diseases.[4,5]

There are a number of technologies that have been reported for the detection of SNPs,[6] such as mass spectrometry,[7,8] electrical detection,[9,10] invasive cleavage[11] and surface enhanced Raman scattering[12] to name a few. Fluorescence based nanodevices capable of detecting SNPs have also been reported, using a chiral peptide nucleic acid and steady state fluorescence,[13] a synthetic DNA oligonucleotide using time-resolved Förster resonance energy transfer,[14] a primer extension genotyping assay using fluorescence depolarisation[15] and a FRET assay using cationic conjugated polymers in homogeneous solution.[16] Presented here is a Holliday junction nanoswitch assay,[17] capable of SNP detection by way of detection of Förster resonance energy transfer (FRET)[18] between two covalently bound fluorophores, demonstrated using a fluorescence lifetime assay in a time-correlated single-photon counting micro plate reader.

The conventional DNA Holliday junction structure, first introduced in 1964, is a junction of four double helices.[19] The distinctive topological element of the junction is the branch point discontinuity formed from covalent bonds at the intersection of the component strands. The overall structure of the junction is determined primarily by the strong electrostatic repulsion between the phosphate groups. Solvated under low ionic strength conditions, this repulsive Coulomb interaction favours an extended structure with maximum charge separation, an open branch point region and approximate four fold symmetry (Fig. 1). This open conformer has also been identified in certain crystal structures of the junction in complexes with recombination and repair proteins.[20]

The DNA Holliday junction sensor assay has two probes, coined A21C-1-1 and A21A-3′, for the detection of a SNP

[a] *School of Physics & Astronomy, James Clerk Maxwell Building, University of Edinburgh, Mayfield Road, Edinburgh, UK EH9 3JZ. E-mail: colin.mcguinness@ed.ac.uk; Fax: +44 (0)131 650 5902; Tel: +44 (0)131 650 5881*
[b] *Division of Pathway Medicine, The Chancellor's Building, University of Edinburgh, 49 Little France Crescent, Edinburgh, UK EH16 4SB*
[c] *National Physical Laboratory, Hampton Road, Teddington, Middlesex, UK TW11 0LW*
† Present address: The Centre for Translational and Chemical Biology, Institute of Structural and Molecular Biology, Michael Swann Building, University of Edinburgh, Mayfield Road, Edinburgh, UK EH9 3JR.

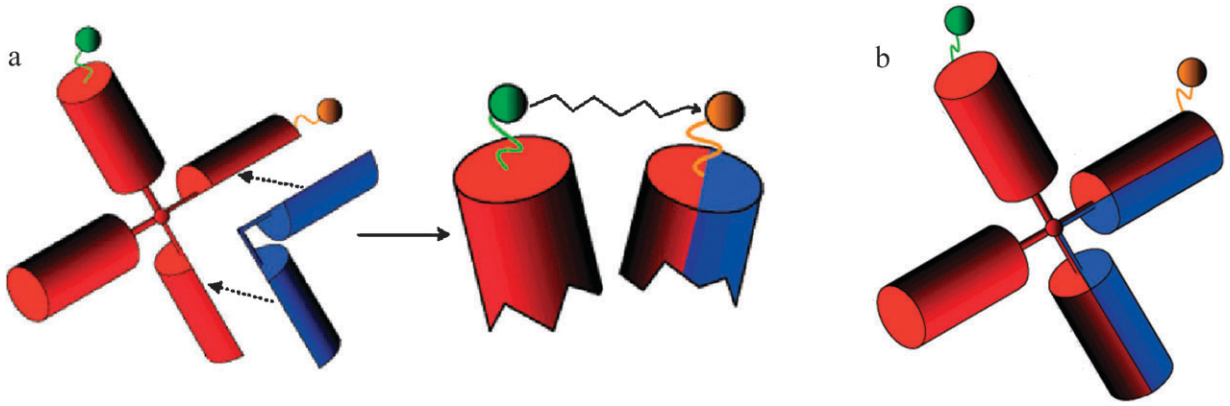

Fig. 1 Schematic diagram of the DNA Holliday junction sensor. The probe (red) binds to the target (blue) by complementary Watson–Crick pairing and the recognition achieved by a conformational change, increasing the FRET between the two fluorophores (a). A schematic of the completed DNA Holliday junction is also shown (b).

located in the human chromosome 11. This SNP has three genotypes depending on the sequence present on each of the two copies of the chromosome: homozygous C (C/C), homozygous A (A/A) or heterozygous (A/C). The probes are designed to distinguish a matched target (C/C with A21C-1-1, A/A with A21A-3′) from a mismatched target.

Experimental methods and analysis

DNA nanoswitch assembly

Two DNA probe sequences were synthesised by Eurogentec Ltd. (Southampton, UK) based on the sequence of an A/C polymorphism at Human Chromosome 11 (NCBI Reference SNP (RefSNP): rs12 270 338). The first probe, A21C-1-1: 5′-CAGAATCCTGAGCACATTTT2GTGCTCACCGAAT-CGGATT1TTCCGATTCGGACTATGGCAT-3′, where the modification "1" refers to the tetramethylrhodamine (TAMRA) fluorophore linked to a thymidine base and modification "2" refers to 6-caroboxyfluorescein (FAM) linked to a thymidine base. The second probe, A21A-3′: 5′-CAGAATCATGAG-CACATTTTGTGCTCACCGAATCGGATT1TTCCGATT-CGGACTATGGCAT-3′, where the modification "1" refers to the TAMRA fluorophore linked to a thymidine base. With A21A-3′, FAM is attached with a C6 linker to the thymidine base at the 3′ end. The value of the critical transfer distance R_0, the distance at which resonance energy transfer is at 50% efficiency, for FAM and TAMRA is 50 Å in solution.[21,22] The synthetic target sequences chosen were 5′-GCCATAGTG-GATTCTG-3′ (perfect match for A21-C-1-1, single base mismatch for A21A-3′) and 5′-GCCATAGTTGATTCTG-3′ (single base mismatch for A21C-1-1, perfect match for A21A-3′). The probe and target were annealed in 20 mM Tris-HCl (pH 7.5), 5 mM $MgCl_2$ and 50 mM NaCl by incubating at 80 °C for 5 min followed by a slow temperature decrease to room temperature. The Mg^{2+} ions were then removed by sequential application to two Sephadex G25 gel filtration columns (Amersham Biosciences UK Ltd., Buckinghamshire, UK) to buffer exchange the samples into 20 mM Tris-HCl (pH 7.5) and 50 mM NaCl. The target was always at 5× excess to ensure full association of probe with target, thus negating the need for consideration of the uncomplexed probe in the analysis.

Measurement and analysis

All fluorescence measurements were carried out at a probe concentration of 100 nM in 96 well black-for-fluorescence microplates (Greiner Bio-One Ltd., Stonehouse, UK) at a sample volume of 100 µl. Fluorescence decays were collected on the Edinburgh Instruments NanoTaurus Fluorescence Lifetime Plate Reader[23] which incorporates the principles of a confocal microscope and utilises the time-correlated single-photon counting technique (TCSPC) for data acquisition. A schematic of the optical components is illustrated in Fig. 2. Data acquisition timing electronics are contained within the Edinburgh Instruments TCC900 PC plug-in card. Donor excitation was achieved using a picosecond pulsed diode laser with nominal wavelength of 470 nm, repetition rate of 10 MHz, and nominal pulse FWHM of ~250 ps. Donor fluorescence was selected using a 35 nm bandpass filter centred at 520 nm. For instrumentation capability verification, decay traces from samples synthesised using different preparation cycles were collected under the conditions of 10 000, 20 000 and 30 000 maximum peak channel counts for all wells. The time resolution for the 10 000 count measurement was 12 ps per channel and 195 ps per channel for the 20 000 and 30 000 count measurements. For a 20 000 peak count measurement, acquisition time was ~5 s per well. In all acquisitions, the fluorescence count rate was ~2% of source repetition rate to avoid the errors in measured decay times associated with photon pile-up.[24] The fluorescence count rate must be significantly low such that for the probability of detecting more than one fluorescence photon per excitation pulse is negligible. If this condition is not met, fluorescence photons will be detected at shorter decay times, thus making the fluorescence decay appear faster than it really is.

All fluorescence decay traces were exported and analysed using a tail-fit global analysis routine. All samples, denoted by x, are assumed to have a level of similarity and are analysed simultaneously. In this case, we assume that the decay of the fluorescence intensities $i(t,x)$ can be represented by a simple sum of exponential components

$$i(t,x) = A(x) + \sum_k B_k(x) \exp\left(-\frac{t}{\tau_k(x)}\right)$$

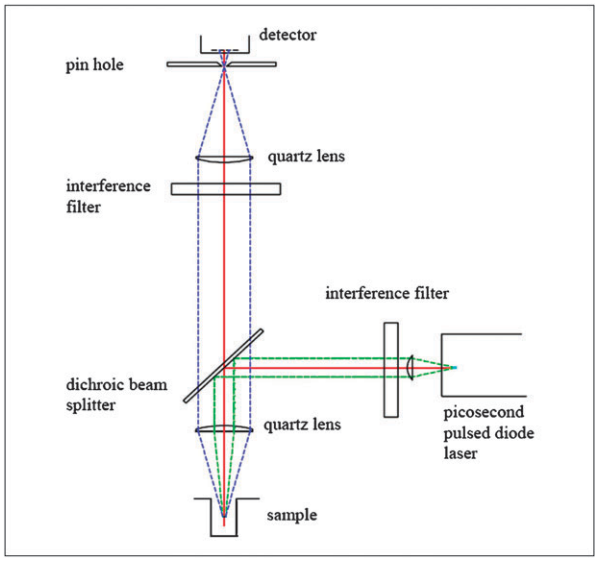

Fig. 2 Schematic diagram of Edinburgh Instruments NanoTaurus micro plate reader optical components.

where A denotes a constant background noise and B_k are the unscaled decay component contributions to the total intensity with corresponding decay time τ_k. This analysis was carried out using Edinburgh Instruments Fluorescence Analysis Software Technology (FAST) Version 2.1.1.

Results and discussion

Global analysis

The decay model chosen for analysing all fluorescence decay traces is one of minimal complexity required to provide a suitable fit. Global analysis is used here, as we are concerned with a system whereby the only measurable difference between the constructs is the fluorophore separation. With a global analysis tail fit, we find two components in $i(t,x)$ with the decay parameter τ_2 linked, but not pre-determined or user constrained, for all traces providing a suitable fit to the data. Linking τ_2 returns a value of 4.1 $\pm$ 0.1 ns for all constructs. This is a reasonable assumption to make in the analysis as the 4.1 ns component is close to the decay time obtained for the donor fluorophore 6-carboxyfluorescein, and in this context, can be attributed to the donor in a highly solvated non-FRET influenced environment. This decay component value has been observed in previous work with the same fluorophore pair covalently bound to the J1 Holliday junction structure.[16] We then assign the decay component τ_1 to the emitted photons that have been influenced by FRET.

Although more components in $i(t,x)$ can be used to improve the fit to the data, one must exercise caution and avoid over-parameterisation. We find, using global analysis, three exponential components in $i(t,x)$ result in over-parameterisation, instability and unphysical negative amplitudes.

The values for decay component τ_1 for the A21C-1-1 and A21A-3′ probes are presented as a histogram with error bars from triplicate measurements and are illustrated in Fig. 3. A matched target for the A21C-1-1 probe is a mismatched target for the A21A-3′ probe and *vice versa*. For the fully complementary matched targets, in both probes, where the junction switching is not inhibited and the FRET is greatest, we observe the shortest value for the τ_1 decay component. Where a base pair mutation is incorporated into the target sequence to give a single base pair mismatch near the junction branch point, we observe a smaller drop in the fluorescence decay component τ_1, indicating weaker FRET and an inhibition of the junction switching. This result is entirely consistent with steady state FRET measurements on mismatches near the branch point,[25] and time-resolved measurements using a femtosecond laser and a traditional TCSPC spectrometer.[26]

With a single well measurement time of <20 seconds and simple tail-fit mathematical analysis of decay components, the advantages of SNP detection using fluorescence lifetime measurements are realised along with acquisition times that are comparable with steady state fluorescence measurements.

Support plane analysis

In addition to the global analysis, confidence level intervals for the calculated parameters were also computed using the support plane analysis option within the discrete components fitting algorithm in FAST Version 2.1.1. The confidence intervals are computed by finding the global minima in the χ^2 error surface and represent the errors of each decay time, taking account of the possible error of one or more of the other fit parameters. Here, we calculate the error intervals for decay components τ_1 for the 20 000 peak channel measurements with decay time τ_2 fixed for the value furnished by the global analysis routine. Using our assumption that the τ_1 decay components represent the FRET influenced emitted photons, we can present the confidence parabolas as fluorophore separation distances according to the following equation, derived from the relationship between the FRET efficiency, separation distance and the decay times with and without acceptor.[27]

$$r = R_0\left(\frac{\tau_1}{\tau_2 - \tau_1}\right)^{\frac{1}{6}}$$

where R_0 is the critical transfer distance of the FRET pair, τ_2 is the unquenched donor decay time (also given by the linked parameter in the global analysis) and r is the fluorophore separation obtained from a particular FRET influenced τ_1 decay component. Assuming two distinct decay components for obtaining donor–acceptor separations has a number of advantages, namely, the components of FRET influenced and uninfluenced photons are separated in the global analysis routine, and it is simply the confidence levels on the FRET influenced components that provide a "distribution" of donor–acceptor separations. Here, no assumption of a form of a distribution, such as a Gaussian, is given and non-FRET influenced photons are not included, thus preventing corruption of the calculated separations.

The fluorophore separations for both A21C-1-1 and A21A-3′ probes are illustrated in Fig. 4. The separations suggest an open–closed (no target no Mg^{2+}, perfect match 5 mM Mg^{2+}) maximum difference in fluorophore separation of around 9 Å

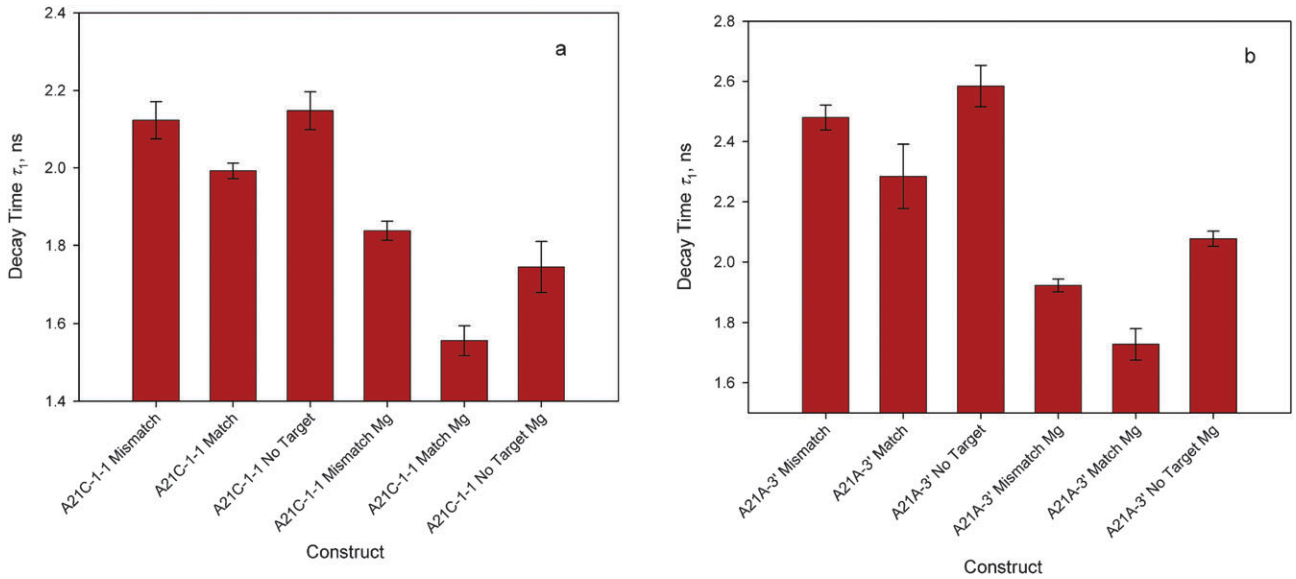

Fig. 3 Histograms of decay component τ_1 obtained from global analysis of decays from A21C-1-1 (a) and A21A-3′ (b) probes with matched, mismatched and no targets, with and without the presence of Mg^{2+} ions. Error bars are standard deviations of measurements in triplicate.

for the A21C-1-1 probe and around 14 Å for the A21A-3′ probe. The upper and lower dashed horizontal lines represent the level of confidence placed upon each separation at 90% and 60%, respectively. Interestingly, for the fully closed constructs, the fluorophore separation obtained for A21C-1-1 is ~49 Å and for A21A-3′, the separation is ~51 Å. This can be explained by the fact that both the donor and acceptor are internally located in the oligonucleotide sequence in the A21C-1-1 probe, whereas only the acceptor is internal for the A21A-3′ probe, with the donor attached with a C6 linker at a thymidine base at the 3′ end and thus gives rise to a slight variation in the separations. Indeed for all target sequences, the separations are slightly larger for the A21C-1-1 probe. If we assume that the fluorophore labelled junction arms are at right angles in the open conformation, the closed conformation fluorophore labelled junction arms form an angle of ~77° for A21C-1-1 and ~71° for A21A-3′.

These confidence intervals provide an additional level of validity to the histograms, in that it provides a reliability estimate on the range of each decay time, taking into account the errors associated with the other fit parameters.

Despite the different approach to the analysis of the fluorescence decays, the separations obtained are within a similar range to those obtained from a similar Holliday junction structure, and fluorophore separations calculated by assuming a Gaussian distribution for the decay times.[17] The fluorophore separation data presented here suggest that a single base pair mismatch in the target sequence gives rise to a 2.5–3 Å increase in the fluorophore separation. This is of the order expected, as previous results calculated using a Gaussian distribution on a range of point mutations near the branch point of a similar Holliday junction[17] give an increase in the fluorophore separation of between 2 and 9 Å. It is also consistent with other work suggesting that non-complementary base sequences disrupt the folding of DNA junctions.[28]

Conclusions

A nucleic acid sensor capable of rapid detection of single nucleotide polymorphisms in clinical samples is introduced. It is based upon the molecular architecture of a branched DNA junction and is demonstrated to be capable of resolving single base mutations in unlabelled target sequences for use in high-throughput plate reader based SNP detection assays. Its operational principles rely on the sensitivity of the conformational energy landscape to base mutations at the branch point. It is therefore a potentially more sensitive discriminator of target mutations than are assays based only on hybridisation energies such as molecular beacons, aptamers and DNAzymes. For example, the molecular beacon's conformational change requires simultaneous formation and breaking of hydrogen bonds under tightly defined conditions, necessitating long assay times.[29] In the device demonstrated here, the probe strands are initially uncomplexed removing any intrinsic energy barrier to hybridisation and can increase the kinetics of detection. This assay also offers the additional advantages of fluorescence lifetime over fluorescence intensity, such as independence of concentration and discrimination against artefacts. These advantages can increase assay reliability and reduce the risk of false hits.

Despite the small structure perturbations involved, the rapid measurement of these perturbations using the time-resolved measurement of the Förster resonance energy transfer between two fluorophores is of sufficient sensitivity to detect single base pair mismatches in synthetic target sequences. The simple mathematical analysis of fluorescence decays also provides a quantitative estimate of the donor–acceptor separations, junction arm angles and the degree of junction switching inhibition caused by single base pair mismatches in a target sequence.

Here, we have demonstrated detection of SNPs at a probe concentration of 100 nM. It is widely accepted that FRET is a

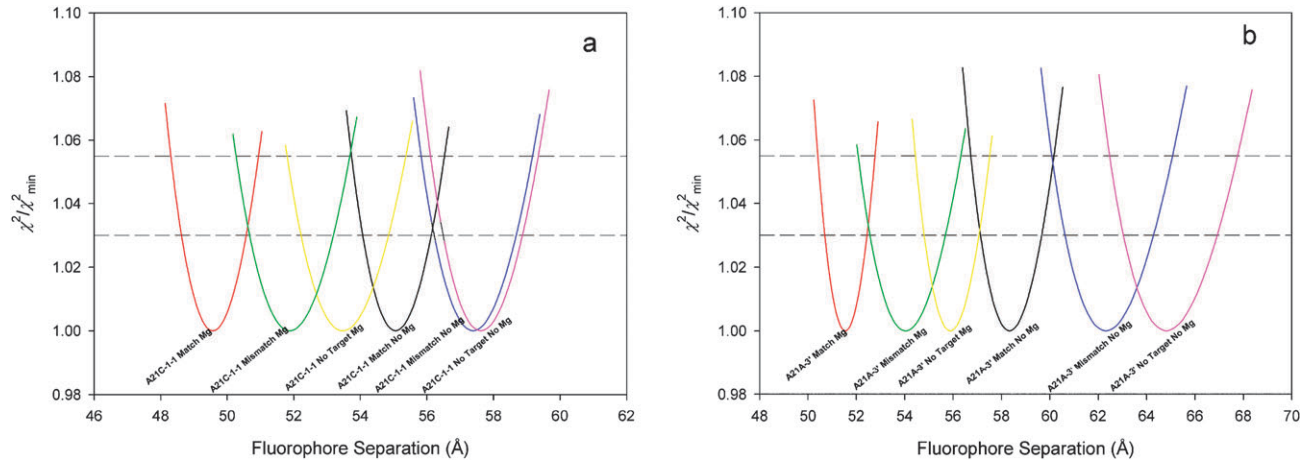

Fig. 4 Confidence levels on the donor–acceptor pair separations for all constructs (with and without Mg^{2+} ions) of the A21C-1-1 (a) and A21A-3′ (b) probes. Upper and lower horizontal dashed lines represent the confidence level at 90% and 60%, respectively.

single molecule level detection technique, and recently the dynamics of RNA folding has been reported, using FRET, with single molecule level of sensitvity.[30] With this in mind, it is conceivable that detection of SNPs using our Holliday junction based sensor will be possible at the single molecule level. With the rapid acquisition of the fluorescence decays, around 8 minutes for a 96 well plate, this sensor design and instrumental architecture provide a real opportunity for short assay times and high-throughput measurement of clinical samples.

Acknowledgements

This work was supported by the Technology Strategy Board under the Fluorescence Lifetime based Assays and Sensors for Healthcare (FLASH) programme.

Notes and references

1 R. P. Hertzberg and A. J. Pope, *Curr. Opin. Chem. Biol.*, 2000, **4**, 445.
2 D. N. Cooper, B. A. Smith, H. J. Cooke, S. Niemann and J. Schmidtke, *Hum. Genet.*, 1985, **69**, 201.
3 F. S. Collins, M. S. Guyer and A. Charkravarti, *Science*, 1997, **278**, 1580.
4 G. C. Johnson and J. A. Todd, *Curr. Opin. Genet. Dev.*, 2000, **10**, 330.
5 N. J. Risch, *Nature*, 2000, **405**, 847.
6 P.-Y. Kwok and X. Chen, *Curr. Issues Mol. Biol.*, 2003, **5**, 43.
7 K. Berlin and I. G. Gut, *Rapid Commun. Mass Spectrom.*, 1999, **13**, 1739.
8 K. H. Buetow, M. Edmonson, R. MacDonald, R. Clifford, P. Yip, J. Kelley, D. P. Little, R. Strausberg, H. Koester, C. R. Cantor and A. Braun, *Proc. Natl. Acad. Sci. U. S. A.*, 2001, **98**, 581.
9 B. A. Cornell, V. L. Braach-Maksvytis, L. G. King, P. D. Osman, B. Raguse, L. Wieczorek and R. J. Pace, *Nature*, 1997, **387**, 580.
10 J. Wang, X. Cai, G. Rivas, H. Shiraishi and N. Dontha, *Biosens. Bioelectron.*, 1997, **12**, 587.
11 J. G. Hall, P. S. Eis, S. M. Law, L. P. Reynaldo, J. R. Prudent, D. J. Marshall, H. T Allawi, A. L. Mast, J. E. Dahlberg, R. W. Kwiatkowski, M. de Arruda, B. P. Neri and V. I. Lyamichev, *Proc. Natl. Acad. Sci. U. S. A.*, 2000, **97**, 8272.
12 B. Moody and G. McCarty, *Anal. Chem.*, 2009, **81**, 2013.
13 F. Totsingan, T. Tedeschi, S. Sforza, R. Corrandini and R. Marchelli, *Chirality*, 2009, **21**, 245.
14 A. Andereoni, M. Bondani and L. Nardo, *Mol. Cell. Probes*, 2009, **23**, 119.
15 X. Chen, L. Levine and P.-Y. Kwok, *Genome Res.*, 1999, **9**, 492.
16 X. Duan, W. Yue, L. Liu, Z. Li, Y. Li, F. He, D. Zhu, G. Zhou and S. Wang, *Nat. Protocols*, 2009, **4**, 984.
17 C. P. Mountford, A. H. Buck, C. J. Campbell, P. Dickinson, E. E. Ferapontova, J. G. Terry, J. S. Beattie, A. J. Walton, P. Ghazal, A. R. Mount and J. Crain, *J. Phys. Chem. B*, 2008, **112**, 2439.
18 T. Förster, *Ann. Phys. (Leipzig)*, 1948, **55**, 437.
19 R. Holliday, *Genet. Res.*, 1964, **5**, 282.
20 D. Hargreaves, D. W. Rucem, S. E. Sedelnikova, P. J. Artymiuk, G. R. Lloyd and J. B. Rafferty, *Nat. Struct. Mol. Biol.*, 1998, **5**, 441.
21 S. D. Lorenz, *Electrophoresis*, 2001, **22**, 990.
22 C. Yuan, E. Rhoades, X. W. Lou and L. A. Archer, *Nucleic Acids Res.*, 2006, **34**, 4554.
23 D. U. Näther, R. Fenske, R. Hurteaux, S. Majno and S. D. Smith, *Proc. SPIE*, 2006, **6372**, 637208.
24 D. J. S. Birch and R. E. Imhof, in *Topics in Fluorescence Spectroscopy Vol. 1: Techniques*, ed. J. R. Lakowicz, Plenum Press, New York, 1991, pp. 1–95.
25 A. H. Buck, C. J. Campbell, P. Dickinson, C. P. Mountford, H. C. Stoquert, J. G. Terry, S. A. G. Evans, L. M. Keane, T.-J. Su, A. R. Mount, A. J. Walton, J. S. Beattie, J. Crain and P. Ghazal, *Anal. Chem.*, 2007, **79**, 4724.
26 M. K. Y. Nishimura, C. D. McGuinness, D. Keszenman-Pererya, P. Dickinson, C. J. Campbell, T. T. Bachmann, P. Ghazal and J. Crain, *Proc. IEEE*, 2009, 1, DOI: 10.1109/SOPO.2009.5230114.
27 J. R. Lakowicz, *Principles of Fluorescence Spectroscopy*, Kluwer Academic/Plenum Publishers, New York, 2nd edn, 2002.
28 D. R. Duckett and D. M. J. Lilley, *J. Mol. Biol.*, 1991, **221**, 147.
29 A. Tsourkas, M. A. Behlke, S. D. Rose and G. Bao, *Nucleic Acids Res.*, 2003, **31**, 1319.
30 Y. Li, X. Qu, A. Ma, G. J. Smith, N. F. Scherer and A. R. Dinner, *J. Phys. Chem. B*, 2009, **113**, 7579.

